Macromolecules
ARTICLE

Macromolecules **2010**, *43*, 9549–9554 **9549**
DOI: 10.1021/ma101441g

Modeling Mesoscale Structure in Comb Polymer Materials for Anhydrous Proton Transport Applications

B. Husowitz and P. A. Monson*

Department of Chemical Engineering, University of Massachusetts, Amherst, Massachusetts 01003, United States

Received June 29, 2010; Revised Manuscript Received October 9, 2010

ABSTRACT: We present Monte Carlo simulation studies of coarse-grained models of some recently developed comb polymers for anhydrous proton transport applications. Our models of the comb polymers incorporate the chain architecture but require only a single χ-parameter for segment−segment interactions. We have studied these models with Monte Carlo simulations using the single chain in mean field (SCMF) method developed by Muller, de Pablo, and co-workers. In these simulations we determine the mesoscale structure and relate it to the polymer architecture in the models. The calculations reveal spontaneous self-assembly of the model comb polymers into mesoscale structures with lamellar or cylindrical symmetries that are similar to those seen in the experiments. The results are also consistent with the picture of the conducting groups concentrating within one of the mesophases, proposed on the basis of the experimental studies. Our calculations also suggest an alternative explanation for the disordered morphologies found in experiments for some of the polymers in terms of the effect of chain branching upon the location of the order−disorder transition.

I. Introduction

The industry standard for proton exchange (or polymer electrolyte) membranes for fuel cells is Nafion.[1] Nafion is an effective proton conductor in its hydrated state but loses this capability at high temperatures when the degree of hydration is greatly reduced.[2] It is naturally worthwhile to investigate other materials that might achieve high rates of proton transport in the anhydrous state, and this has been the subject of several recent investigations.[3−7] In particular, a recent study by our colleagues on the properties of a series of N-heterocycle-functionalized comb polymers indicated that some of these polymers exhibit substantially elevated proton conductance.[7] Moreover, structural characterization of the materials provided evidence of mesoscale structure that might facilitate transport via high concentration of the proton conducting functionalities within cylindrical or lamellar mesophases.[7] The four polymers discussed in that paper are shown in Figure 1, and we refer to these as polymers A through D. They are comb polymers consisting of a polystyrene backbone to which conducting groups are attached via a flexible side chain.

Two of the polymers feature benzotriazole conducting groups while the other two feature imidazole conducting groups. The conducting groups are attached at the meta position to the styrene via a flexible connecting group. The addition of an extra alkoxy substituent at the other meta position on the styrene (polymers B and D) makes a substantial difference to the material properties. Polymers B and D are found to have much higher conductivities relative to polymers A and C, which do not have the extra alkoxy substituent. In addition, structural characterization revealed disordered morphologies for polymers A and C while polymers B and D exhibited mesoscale order, with the conducting groups concentrated in lamellar and cylindrical mesophases, respectively. These results highlight the potential for making anhydrous proton conducting materials that exploit the mesoscale structural characteristics of branched polymers. The purpose of the present paper is to provide additional insights into these observations from Monte Carlo simulation studies of coarse-grained models of the comb polymers, in which we determine the mesoscale structure and relate it to the polymer architecture. Before describing our work in more detail, we provide additional context with a brief review of some key results on experiment and modeling of mesoscale structures in comb polymers.

The molecular architecture of polymers has been recognized as an important factor in determining the morphology at the mesoscale. The best known example of this, diblock copolymers, have been investigated extensively, and various morphologies from lamellae to cylinders to bicontinuous structures such as gyroids have been observed.[8,9] The morphology of such copolymers is controlled by the compatibility of the blocks and the volume fraction of the different monomer species. The mesophase structures that form reflect a delicate balance between the interaction energy between chains and the chain stretching energy.[10] For diblocks the repulsion between chemically different species gives rise to phase separation, and since the blocks are connected, the system exhibits microphase separation rather than macrophase separation. The extension of these ideas to branched polymers is of significant interest, particularly in the context of developing nanostructured materials for various functional materials applications.[11,12] Systematic investigations of mesoscale morphology for branched copolymers have been made by Gido and co-workers, for instance.[13−19] They synthesized a series of grafted and multigrafted copolymers with different polymer architectures and determined that the number of grafts and the distributions of junction points greatly affects the microphase separation. Well-ordered lamellae, spherical micelles, and cylindrical phases were observed, depending on the architecture.

Various theoretical studies have been conducted on grafted copolymers.[20−27] Many of these studies have focused on how the number of graft points and the location of the graft points affect

*Corresponding author. E-mail: monson@ecs.umass.edu.

Published on Web 10/26/2010

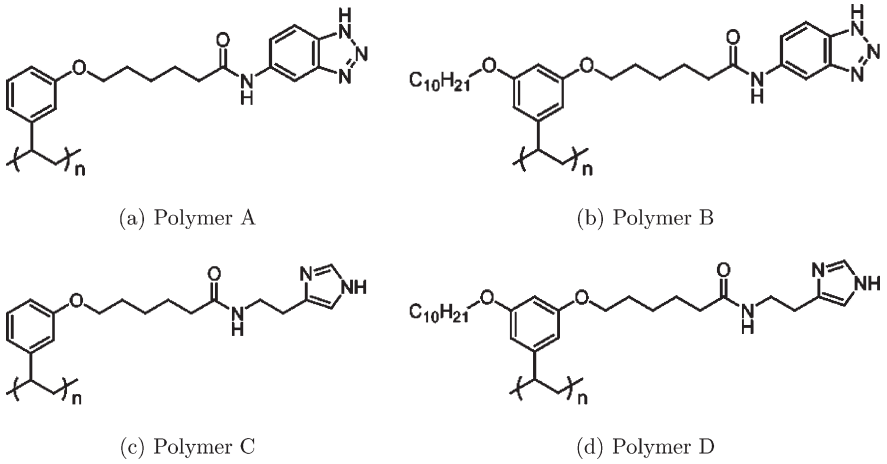

Figure 1. Chemical structures of the polymers studied by Chen et al.[7] The first two polymers, A and B, both have a benzotriazole proton conducting group while the second two polymers, C and D, have an imidazole proton conducting group. In each case for one of the polymers with the same proton conducting group an additional alkyl chain has been added to the ortho position of the styrene ring, B and D.

the morphology and the order to disorder phase transition. Recently, Zhang et al.[28] examined phase diagrams for graft copolymers in three dimensions as a function of the number of graft points and the position of the first junction point. Using self-consistent field theory (SCFT), it was determined that the phase diagrams were asymmetric as compared with diblocks. In addition, the number of graft points and position of the first graft point were found to shift the phase boundaries. In a previous study using SCFT in two dimensions, they also showed that by changing the number of graft points and the location of the first graft point a lamellar to cylindrical morphological change is observed.[29] Theoretical studies of double-grafted copolymers have also been made. In particular, Palyulin et al.[30] studied the microphase separation of double-grafted copolymers with gradient, random, and regular sequence of the branch points. Wang et al.[27] found that the order−disorder transition (ODT) for comb polymers from SCFT was shifted to higher χ-parameter with increasing number of side chains. This is consistent with earlier theoretical observations of a shift in the ODT to lower temperatures for more complex polymer melts.[31,32] Such effects have also been seen experimentally in comparison of star polymers[33] and comb polymers with diblock copolymers.[34]

In this paper we focus on modeling the properties of the four comb polymers shown in Figure 1. We have constructed simple coarse-grained models of these polymers that incorporate the broad features of the chain architecture while requiring only a single χ-parameter for segment−segment interactions. We have studied these models with Monte Carlo simulations using the single chain in mean field (SCMF) method developed by Muller, de Pablo, and co-workers.[35,36] We find that this method allows us to study the spontaneous self-assembly of the model comb polymers from initial disordered states into mesophase structures with lamellar or cylindrical symmetries consistent with those seen in the experimental results.[7] Our calculations also suggest an explanation for the disordered morphologies found experimentally for polymers A and C in Figure 1.

In the next section we describe the coarse-grained models and the essentials of the SCMF method. In section III we present our results for the structural properties of the model polymers. Section IV gives a summary of our results and conclusions.

II. Model and Simulation Methodology

Our modeling approach closely follows that of Muller, de Pablo, and co-workers.[35,36] We consider a minimal coarse-grained model that includes the chain architecture and interchain interactions at the level of a mean field energy functional. We represent the polymers as interacting segments, and the coarse-graining schemes for the polymers shown in Figure 1 are shown in Figure 2. We identify two kinds of segments, 1 (black beads) and 2 (gray beads), corresponding to nonconducting groups and conducting groups, respectively.

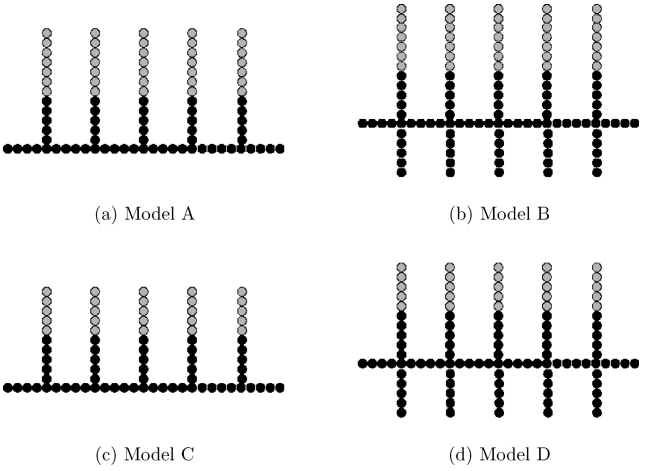

Figure 2. Coarse-grained models of the polymers shown in Figure 1 with proton conducting groups (light gray beads) and nonconducting groups (black beads). The bulkier benzotriazole group is represented by seven beads while the smaller imidazole group is represented by five beads, while in both cases the additional alkyl chain consisting of five beads.

The distribution of the segment types in the model is intended to reflect roughly the sizes of the different groups in the real polymers. This coarse graining is arguably oversimplified, but it has the advantage that we need only a single χ-parameter in the model. We believe it appropriate for the primarily qualitative study of the phenomenology undertaken in this work. We also note that it is in the same spirit as coarse-grained models of Nafion that have been used in recent work.[37−40] Moreover, it is a simple realization of the physics underlying the mesoscale structure suggested by Chen et al.[7] for their comb polymer systems. We will refer to the models illustrated in Figure 2 as models A through D, in keeping with our labeling of the actual polymers in Figure 1. The representation of the conducting side chains as diblocks, inspired by some models of Nafion,[37,39,40] may not be necessary. The major feature of the self-assembly in these systems is the phase separation between the conducting groups and the

backbone and how this is modified by additional alkyl side chains. However, changing the conducting side chains from diblocks to single blocks is unlikely to affect the qualitative results.

To describe the energy of the model system, we first write the Hamiltonian in terms of bonded and nonbonded interactions involving the representation of the polymer by interacting segments via

$$H = H_b + H_{nb} \tag{2.1}$$

H_b is modeled via the discrete Edwards Hamiltonian or Gaussian chain so that for a polymer with N segments we have

$$H_b = \sum_{i=1}^{n}\sum_{s=1}^{N-1}\frac{3}{2b^2}[\mathbf{r}_i(s)-\mathbf{r}_i(s+1)]^2 \tag{2.2}$$

where b is the average bond length between each segment and $\mathbf{r}_i(s)$ is the coordinate of segment s of chain i. For the nonbonded interactions we write[36]

$$\frac{H_{nb}[\phi_1(\mathbf{r}),\phi_2(\mathbf{r})]}{k_bT} = \frac{\rho}{N}\int_V d^3\mathbf{r}\left[\frac{\kappa N}{2}[\phi_1(\mathbf{r})+\phi_2(\mathbf{r})-1]^2+\chi N\phi_1(\mathbf{r})\phi_2(\mathbf{r})\right] \tag{2.3}$$

where $\rho = nN/V$ denotes the segment number density (n is the number of chains and N is the number of segments per chain) and $\phi_J(\mathbf{r})$ is the local volume fraction of species J. κ is proportional to the inverse compressibility of the liquid, and χ describes the repulsion between coarse-grained segments. This contribution to the Hamiltonian has the form of a mean-field energy functional incorporating repulsions between unlike segments as in the Flory–Huggins theory and the modeling of incompressibility via the Helfand–Tagami quadratic model.[41,42]

To understand the SCMF method, it is instructive to rewrite eq 2.3 as

$$\frac{H_{nb}[\phi_1(\mathbf{r}),\phi_1(\mathbf{r})]}{k_bT} = \frac{\rho}{2N}\int_v d^3\mathbf{r}\,[w_1(\mathbf{r})\phi_1(\mathbf{r})+w_2(\mathbf{r})\phi_2(\mathbf{r})] \tag{2.4}$$

where

$$w_1(\mathbf{r}) = \kappa N[\phi_1(\mathbf{r})+\phi_2(\mathbf{r})-1]+\chi N\phi_2(\mathbf{r}) \tag{2.5}$$

and

$$w_2(\mathbf{r}) = \kappa N[\phi_1(\mathbf{r})+\phi_2(\mathbf{r})-1]+\chi N\phi_1(\mathbf{r}) \tag{2.6}$$

From eq 2.4 we see that the interaction energy can be expressed in terms of fields $w_1(\mathbf{r})$ and $w_2(\mathbf{r})$ acting on the type 1 and type 2 segments of the polymer chains, respectively. Of course, these fields actually depend upon both local volume fractions as shown in eqs 2.5 and 2.6.

In discretized form eq 2.4 can be expressed as

$$\frac{H_{nb}[\phi_1,\phi_2]}{K_BT} = \frac{\rho\Delta L^3}{2N}\sum_{m=1}^{N_{cells}}(w_{1,m}\phi_{1,m}+w_{2,m}\phi_{2,m}) \tag{2.7}$$

This expression is based on dividing the system on a simple cubic grid with N_{cell} cells and a grid size ΔL. A Monte Carlo simulation of this kind of model is readily achieved by moving the polymers in the fields and using eq 2.7 to calculate the energy. To do this without further approximation, the effect upon the fields of moving a chain must be included in determining the acceptance probabilities for the new configuration in the Monte Carlo simulation and the fields updated after each successful chain move.[43] The essence of the SCMF method[35,36] is to approximate the Monte Carlo simulation by only updating the fields at set intervals. In this work we update the fields after each Monte Carlo step (i.e., an attempt to move each polymer in the system).

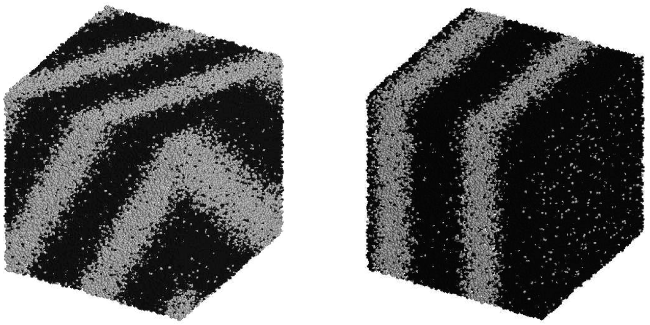

Figure 3. Computer graphics visualizations of states from our models of the benzotriazole polymers. Left: polymer A with $\chi = 1.40$. Right: polymer B with $\chi = 1.80$. The simulation cell is $32b \times 32b \times 32b$.

In our SCMF simulations we considered system sizes mostly of $32b \times 32b \times 32b$ and in some cases $64b \times 64b \times 64b$, with all systems in periodic boundaries. The segment density used was $\rho b^3 = 21.57$; we used a fixed value of $\kappa = 1.5625$, based on values used in previous work with the SCMF method,[35,36] and we fixed the grid size at $\Delta L = b$. With the given parameters these simulations typically involve several hundred thousand segments, but due to the structure of the SCMF method, they run much more quickly than simulations with explicit particle–particle interactions. We initiated our simulations from a state where the polymers were randomly distributed with the conformations shown in Figure 2. The Monte Carlo moves used were single segment displacement, whole polymer displacement moves, and reptation moves. After initiating the system, we ran a simulation with $\chi = 0$ for 10^5 Monte Carlo steps to generate an initial disordered polymer configuration. After that, the χ-parameter was increased and the simulation was run until there appeared to be no further change in the morphology, as observed in computer graphics visualizations. This typically required about 2×10^5–4×10^5 additional Monte Carlo steps. For some of the runs we also obtained the average of the structure factor of composition fluctuations for comparison with results from scattering experiments.[7] We have

$$S(q) = \frac{1}{4nN}\langle|\sum_{j=1}^{n}\sum_{s=1}^{N}[\gamma_1(s)-\gamma_2(s)]e^{-i\mathbf{q}\cdot\mathbf{r}_j(s)}|^2\rangle \tag{2.8}$$

where $\gamma_J(s)$ is unity if segment s is of type J and zero otherwise. As an initial check on the application of the SCMF method to branched polymers, we began by testing the method for some of the systems studied using SCFT.[29,28] We found that we could reproduce the trends found in those studies. For instance, we found that increasing the spacing between side chains in a comb polymer with type 1 backbone segments and type 2 side chains led to a change from lamellar to cylindrical mesophase structure.

III. Results

We begin by considering the results for our models of the benzotriazole polymers A and B. Figure 3 shows computer graphics visualizations of the equilibrated configurations for the models A and B. We see a lamellar structure in both cases.

The conducting groups are concentrated in the gray phase and the nonconducting groups in the black phase. We have found that the ODT is moved to higher χ by the additional alkoxy substituent, and this is consistent with other calculations on comb polymers[27] as well as earlier theoretical work on the effect of departures from linear chain architectures on the ODT.[31−33] The origin of this behavior is that more branching in the polymers leads to a greater loss in configuration space upon creating ordered structures so that the interaction energies have to be greater in order to drive the system into an ordered state.

At first glance it appears that our results are inconsistent with experiment in that no evidence of mesoscale ordering was found in the experimental scattering measurements for the polymer A, whereas our calculations predict a lamellar structure for both the model polymers A and B. We suspect that this difference is related to the effect of chain branching on the ODT that we just mentioned. If we simulate model A at a higher value of χ, then we find that with the set of Monte Carlo moves we are using the system fails to equilibrate and becomes frozen into an essentially disordered structure with some phase separation only at small length scales. This is shown in Figure 4. This failure to equilibrate is likely related to the increased roughness of the energy landscape for the model as we increase χ. When polymer A is simulated at a higher value of χ beyond the ODT for the polymer B, this represents a still deeper quench into the two-phase region for polymer A. The energy landscape for model A becomes rougher, leading to the very slow dynamics. We have repeated the calculation of this system using a finer chain discretization, using double the value of N while preserving the values of χN and κN,[35] and the same behavior is observed. The observation of very slow dynamics here may well be related to a similar phenomenon observed for linear diblock copolymers, as discussed by Zhang and Wang.[44] Indeed, in some test simulations of linear diblocks with the SCMF method we have found the same arrested kinetics upon quenching to large values of χ.

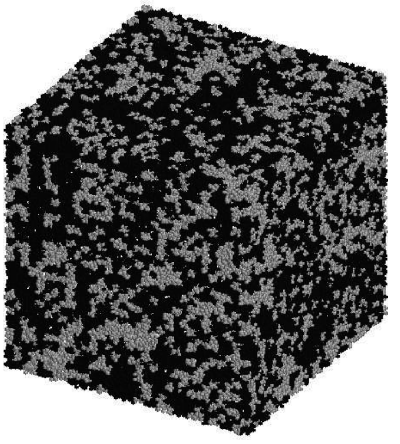

Figure 4. Computer graphics visualizations of state from model A (benzotriazole polymer without additional alkoxy side chain) with χ = 1.80. The system fails to equilibrate and exhibits a disordered structure with only small scale phase separation.

The structure factors for our ordered and disordered states for models A and B are compared with experiment in Figure 5. For the ordered structures the important points of comparison are the relative locations of two peaks apparent in each case. We find that in both cases $q_2/q_1 \sim \sqrt{4}$ as expected for a lamellar structure. Close quantitative agreement between the model and experiment should not be expected since, in addition to questions of the model validity, the experimental results represent an average over a much larger sample in which there are structured domains with different orientations, whereas the simulations of the model are for a small and oriented sample of the morphology.

We turn now to the comb polymer with the imidazole conducting group (polymers and models C and D). Figure 6 shows computer graphics visualizations of equilibrated configurations for the model polymers. In this case we see a transition from a lamellar structure without the alkoxy substituent to a cylindrical one with this substituent. This is consistent with results from earlier studies of branched polymers.[27]

The change of morphology to a cylindrical one can be interpreted as follows. It can be seen as arising from a dilution effect associated with the lower fraction of the conducting groups when the extra side chain is added. Under these circumstances it is not possible to have a sample spanning phase of the conducting groups arranged in a lamellar structure, but it is if they are arranged in cylinders. Also, the addition of the extra side chain leads to crowding at the 1−2 interface which is relieved by curvature.[10] The dilution effect does not happen for our model of the comb polymer with the benzotriazole groups, model B, because these groups are larger and sample spanning lamellae can still be achieved even with the extra side chain. In addition, the crowding of the larger benzotriazole groups also acts to oppose the cylinder formation. The cylindrical morphology seen for model D is consistent with what is seen in the experiments, but again we have the prediction of an ordered morphology for the polymer without the extra alkoxy group, model C. We have again seen the effect of the extra side chain in moving the ODT to higher χ values for models C and D. Also, when model C is studied at higher χ values, comparable to that where ordered structures are seen for model D, we again observe the formation of frozen disordered domains without equilibration similar to that seen in Figure 4. The structure factors for our ordered and disordered states for models C and D are compared with experiment in

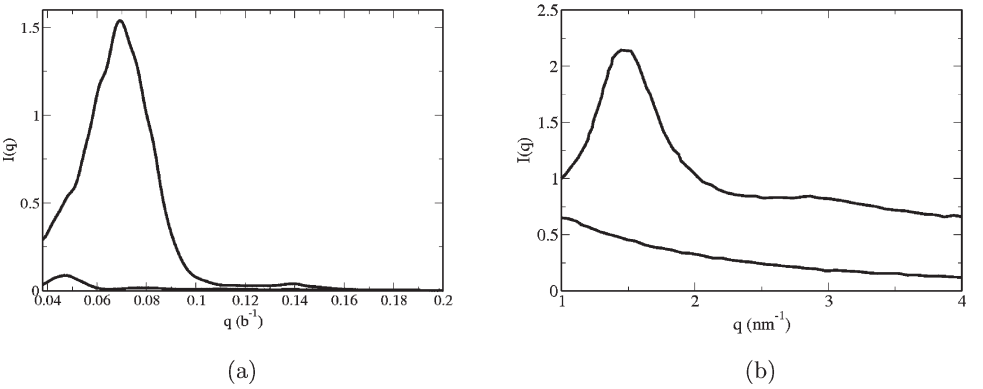

Figure 5. Structure factors from simulation (left) and experiment (right) for the benzotriazole polymers showing the results from the lamellar and disordered mesoscale structures. For each graph the upper curve corresponds to polymer B and the lower curve to polymer A.

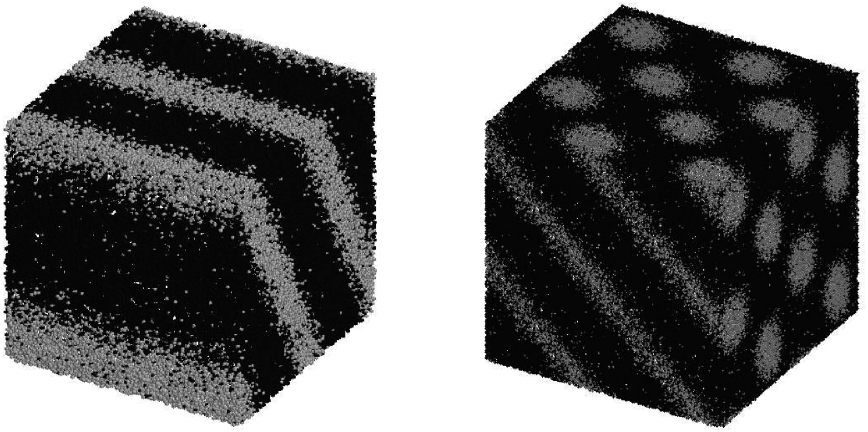

(a) (b)

Figure 6. Computer graphics visualizations of states from our models of the imidazole polymers. Left: model C with $\chi = 1.40$. Right: model D with $\chi = 1.80$. The simulation cell size for model C is $32b \times 32b \times 32b$, and for model D it is $64b \times 64b \times 64b$.

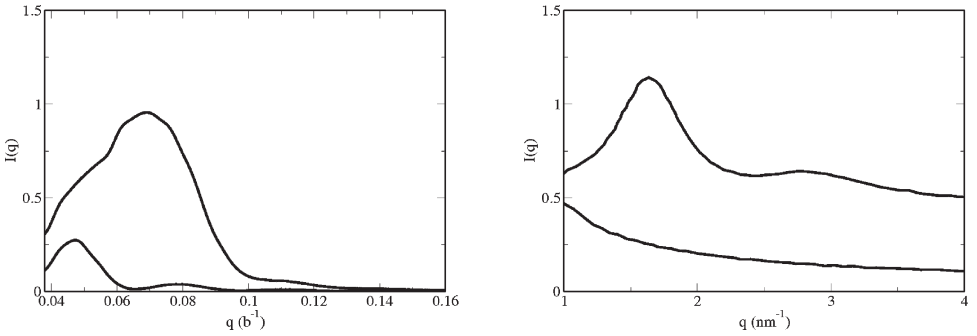

(a) (b)

Figure 7. Structure factors from simulation (top) and experiment (bottom) for the imidazole polymers showing the results from the cylindrical and disordered mesoscale structures. For each graph the upper curve corresponds to polymer D and the lower curve to polymer C.

Figure 7. In this case the ratio of the two peak locations $q_2/q_1 \sim \sqrt{3}$, which is indicative of a cylindrical morphology in both the theoretical and experimental results.

IV. Summary and Conclusions

We have presented a Monte Carlo simulation study using the SCMF method[35,36] of coarse-grained models of comb polymers for anhydrous proton conduction applications. Our calculations predict the formation of lamellar and cylindrical morphologies which were seen experimentally for some of these polymers.[7] The formation of cylindrical rather than lamellar structures in one case (model D) is consistent with earlier theoretical studies of comb polymer systems.[27]

In contrast to the experimental situation, our models of all four comb polymers exhibit ordered mesoscale structures. In the experiments the polymers without the additional alkoxy side chains (polymers A and C) exhibited disordered structures.[7] Chen et al.[7] offer an explanation for this in terms of a decreased compatibility between the conducting groups and the rest of polymer upon the addition of the extra side chain. They argue that this would lead to enhanced mesophase segregation of the conducting and nonconducting groups. Our results suggest an alternative explanation related to the effect of chain branching upon the ODT. We find that the ODT transition for the polymers without the additional side chain (A and C) lies at a lower value of χ than for polymers B and D. When polymers A and C are simulated at a higher value of χ beyond the ODT's for polymers B and D, this represents a much deeper quench into the two-phase region for these polymers. The energy landscape becomes rougher and the systems fail to equilibrate, becoming frozen in states with only slight phase separation in small scale domains.

Further investigation of this slow dynamics would be worthwhile. For instance, experimental studies of the morphologies for polymers A and C at higher temperatures might be useful. Another interesting investigation would be to use simulations to study the evolution of the morphologies during solvent casting processes similar to those used to prepare samples for the experimental scattering and conductivity measurements. It would also be useful to make further calculation with the present model to observe the time evolution of order parameters associated with the phase separation and to explore the relationship with similar phenomena in linear diblock systems.[44] Finally, it would be interesting to see if the slow relaxation process is also seen in calculations of these kinds of systems via dissipative particle dynamics for related coarse-grained models.[45,46]

The results of this study indicate that the SCMF method is useful for studying the mesoscopic self-assembly for branched polymers. We are currently using it to study other branched and network polymer systems for proton transfer applications.

Acknowledgment. This work was supported by the National Science Foundation Center for Chemical Innovation, "Fueling the Future", at the University of Massachusetts (Grant No. 0739227). We are grateful to S. Christensen and R. Hayward for providing us with their scattering data for the proton conducting comb polymers.[7] We thank the referees for several useful suggestions, including directing us to the work of Zhang and Wang.[44]

References and Notes

(1) Mauritz, K.; Moore, R. *Chem. Rev.* **2004**, *104*, 4535–4585.
(2) Hickner, M.; Ghassemi, H.; Kim, Y.; Einsla, B.; McGrath, J. *Chem. Rev.* **2004**, *104*, 4587–4611.
(3) Granados-Focil, S.; Woudenberg, R. C.; Yavuzcetin, O.; Tuominen, M. T.; Coughlin, E. B. *Macromolecules* **2007**, *40*, 8708–8713.
(4) Persson, J.; Jannasch, P. *Macromolecules* **2005**, *38*, 3283–3289.
(5) Scharfenberger, G.; Meyer, W. H.; Wegner, G.; Schuster, M.; Kreuer, K. D.; Maier, J. *Fuel Cells* **2006**, *6*, 237–250.
(6) Zhou, Z.; Li, S.; Zhang, Y.; Liu, M.; Li, W. *J. Am. Chem. Soc.* **2005**, *127*, 10824–10825.
(7) Chen, Y.; Thorn, M.; Christensen, S.; Versek, C.; Poe, A.; Hayward, R.; Tuominen, M.; Thayumanavan, S. *Nature Chem.* **2010**, *2*, 503–508.
(8) Bates, F.; Fredrickson, G. *Phys. Today* **1999**, *52*, 32.
(9) Fredrickson, G.; Bates, F. *Annu. Rev. Mater. Sci.* **1996**, *26*, 501.
(10) Milner, S. *Macromolecules* **1994**, *27*, 2333.
(11) Ikkala, O.; ten Brinke, G. *Science* **2002**, *295*, 2407.
(12) Forster, S.; Konrad, M. *J. Mater. Chem.* **2003**, *13*, 2671.
(13) Gido, S.; Lee, C.; Pochan, D.; Pispas, S.; Mays, J.; Hadjichristidis, N. *Macromolecules* **1996**, *29*, 7022–7028.
(14) Gido, S.; Wang, Z. *Macromolecules* **1997**, *30*, 6771–6782.
(15) Lee, C.; Gido, S.; Poulos, Y.; Hadjichristidis, N.; Tan, N.; Trevino, S.; Mays, J. *J. Chem. Phys.* **1997**, *107*, 6460.
(16) Lee, C.; Gido, S.; Poulos, Y.; Hadjichristidis, N.; Tan, N.; Trevino, S.; Mays, J. *Polymer* **1998**, *39*, 4631.
(17) Beyer, F.; Gido, S.; Buschl, C.; Iatrou, H.; Uhrig, D.; Mays, J.; Chang, M.; Garetz, B.; Balsara, N.; Tan, N.; Hadjichristidis, N. *Macromolecules* **2000**, *33*, 2039.
(18) Weidisch, R.; Gido, S.; Uhrig, D.; Iatrou, H.; Mays, J.; Hadjichristidis, N. *Macromolecules* **2001**, *34*, 6333.
(19) Mays, J.; Uhrig, D.; Gido, S.; Zhu, Y.; Weidisch, R.; Iatrou, H.; Hadjichristidis, N.; Hong, K.; Beyer, F.; Lach, R.; Buschnakowski, M. *Macromol. Symp.* **2004**, *215*, 111.
(20) Delacruz, M.; Sanchez, I. *Macromolecules* **1986**, *19*, 2501.
(21) Shinozaki, A.; Jasnow, D.; Balazs, A. *Macromolecules* **1994**, *27*, 2496.
(22) Israels, R.; Foster, D.; Balazs, A. *Macromolecules* **1995**, *28*, 218.
(23) Qi, S.; Chakraborty, A.; Wang, H.; Lefebvre, A.; Balsara, N.; Shakhnovich, E.; Xenidou, M.; Hadjichristidis, N. *Phys. Rev. Lett.* **1999**, *82*, 2896.
(24) Qi, S.; Chakraborty, A. *J. Chem. Phys.* **2001**, *115*, 3401.
(25) Patel, D.; Fredrickson, G. *Phys. Rev. E* **2003**, *68*, 051802.
(26) Ye, X.; Shi, T.; Lu, Z.; Zhang, C.; Sun, Z. *Macromolecules* **2005**, *38*, 8853.
(27) Wang, R.; Jiang, Z.; Hu, J. *Polymer* **2005**, *46*, 6201.
(28) Zhang, L.; Lin, J.; Lin, S. *J. Phys. Chem. B* **2008**, *112*, 9720.
(29) Zhang, L.; Lin, J.; Lin, S. *J. Phys. Chem. B* **2007**, *111*, 351.
(30) Palyulin, V. V.; Potemkin, I. I. *J. Chem. Phys.* **2007**, *127*, 124903.
(31) Marko, J. *Macromolecules* **1993**, *26*, 1442.
(32) Benoit, H.; Hadziioannou, G. *Macromolecules* **1988**, *21*, 1449.
(33) Buzza, D.; Hamley, I.; Fzea, A.; Moniruzzaman, M.; Allgaier, J.; Young, R.; Olmsted, P.; McLeish, T. *Macromolecules* **1999**, *32*, 7483.
(34) Chiang, W.; Lin, C.; Nandan, B.; Yeh, C.; Rahman, M.; Chen, W.; Chen, H. *Macromolecules* **2008**, *41*, 8138–8147.
(35) Daoulas, K. C.; Muller, M. *J. Chem. Phys.* **2006**, *125*, 184904.
(36) Daoulas, K. C.; Muller, M.; de Pablo, J. J.; Nealey, P. F.; Smith, G. D. *Soft Matter* **2006**, *2*, 573.
(37) Galperin, D.; Khokhlov, A. *Macromol. Theory Simul.* **2006**, *15*, 137–146.
(38) Wescott, J.; Qi, Y.; Subramanian, L.; Capehart, T. *J. Chem. Phys.* **2006**, *124*, 134702.
(39) Wu, D.; Paddison, S. J.; Elliott, J. A. *Energy Environ. Sci.* **2008**, *1*, 284–293.
(40) Wu, D.; Paddison, S. J.; Elliott, J. A. *Macromolecules* **2009**, *42*, 3358–3367.
(41) Helfand, E.; Tagami, Y. *J. Polym. Sci., Polym. Lett.* **1971**, *9*, 741.
(42) Helfand, E.; Tagami, Y. *J. Chem. Phys.* **1972**, *57*, 1812.
(43) Detcheverry, F. A.; Kang, H.; Daoulas, K. C.; Mueller, M.; Nealey, P. F.; de Pablo, J. J. *Macromolecules* **2008**, *41*, 4989–5001.
(44) Zhang, C.; Wang, Z. *Phys. Rev. E* **2006**, *73*, 031804.
(45) Martinez-Veracoechea, F. J.; Escobedo, F. A. *Macromolecules* **2009**, *42*, 1775–1784.
(46) Martinez-Veracoechea, F. J.; Escobedo, F. A. *J. Chem. Phys.* **2006**, *125*, 104907.